Supplementary Information

Manganese enhances macrophage bactericidal activity in mice with *Staphylococcus aureus* osteomyelitis via Sirt3-mitophagy axis

Xin Guan[1,2#], Bingsheng Yang[3#], Bowen Bai[4#], Naiqian Cui[4], Muqi Wang[4], Jianwen Su[4], Xiaohu Wu[5], Chenghua Zhang[4], Hui Dai[6], Peng Zhao[7,8,9†], Bin Yu[1,2,4†], Bowei Wang[10,11†]

1. Pingshan Hospital, Southern Medical University, Shenzhen, China.
2. Pingshan District Peoples' Hospital of Shenzhen, Shenzhen, China.
3. Department of Joint and Orthopedics, Zhujiang Hospital, Southern Medical University, Guangzhou, China.
4. Guangdong Provincial Key Laboratory of Bone and Cartilage Regenerative Medicine, Nanfang Hospital, Southern Medical University, Guangzhou, China.
5. Department of Orthopedic Trauma and Arthroplasty, The Affiliated Traditional Chinese Medicine Hospital, Guangzhou Medical University, Guangzhou, China.
6. Ganzhou Hospital-Nanfang Hospital, Southern Medical University, Ganzhou, China.
7. School of Pharmaceutical Sciences, Southern Medical University, Guangzhou, China.
8. Guangdong Provincial Key Laboratory of New Drug Screening, Southern Medical University, Guangzhou, China.
9. NMPA Key Laboratory for Research and Evaluation of Drug Metabolism, Southern Medical University, Guangzhou, China.
10. Department of Trauma Emergency Center, Ganzhou Hospital-Nanfang Hospital, Southern Medical University, Ganzhou, China.
11. Division of Orthopaedics and Traumatology, Department of Orthopaedics, Nanfang Hospital, Southern Medical University, Guangzhou, China.

†Corresponding authors. E-mail addresses: hellobowei@hotmail.com (Bowei Wang), 81297810@qq.com (Bin Yu), smuzp@smu.edu.cn (Peng Zhao).

#Authors contributed equally to this work.

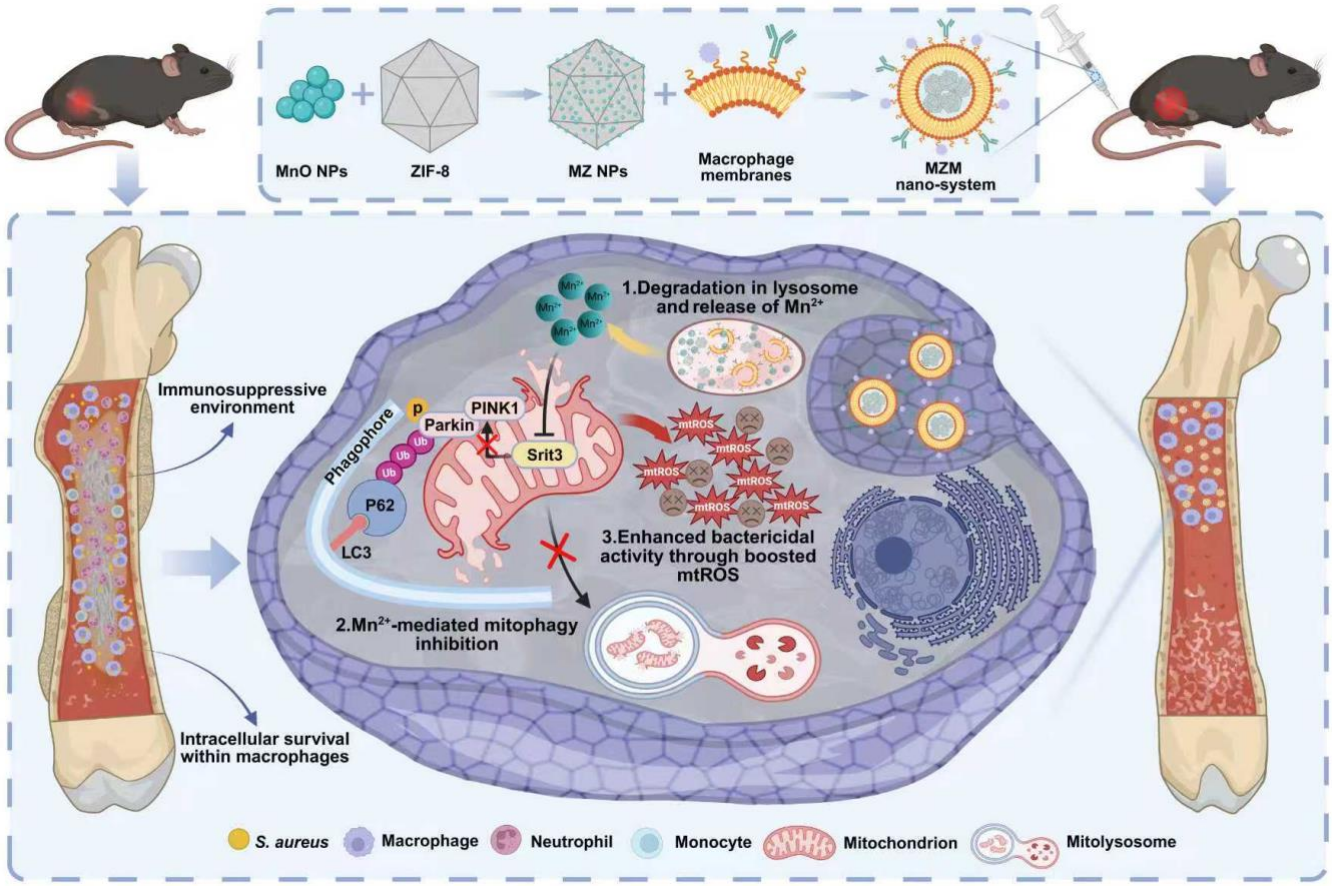

Supplementary Schematic illustration. created in BioRender. Kwan, O. (2026) https://BioRender.com/b5ukyj5

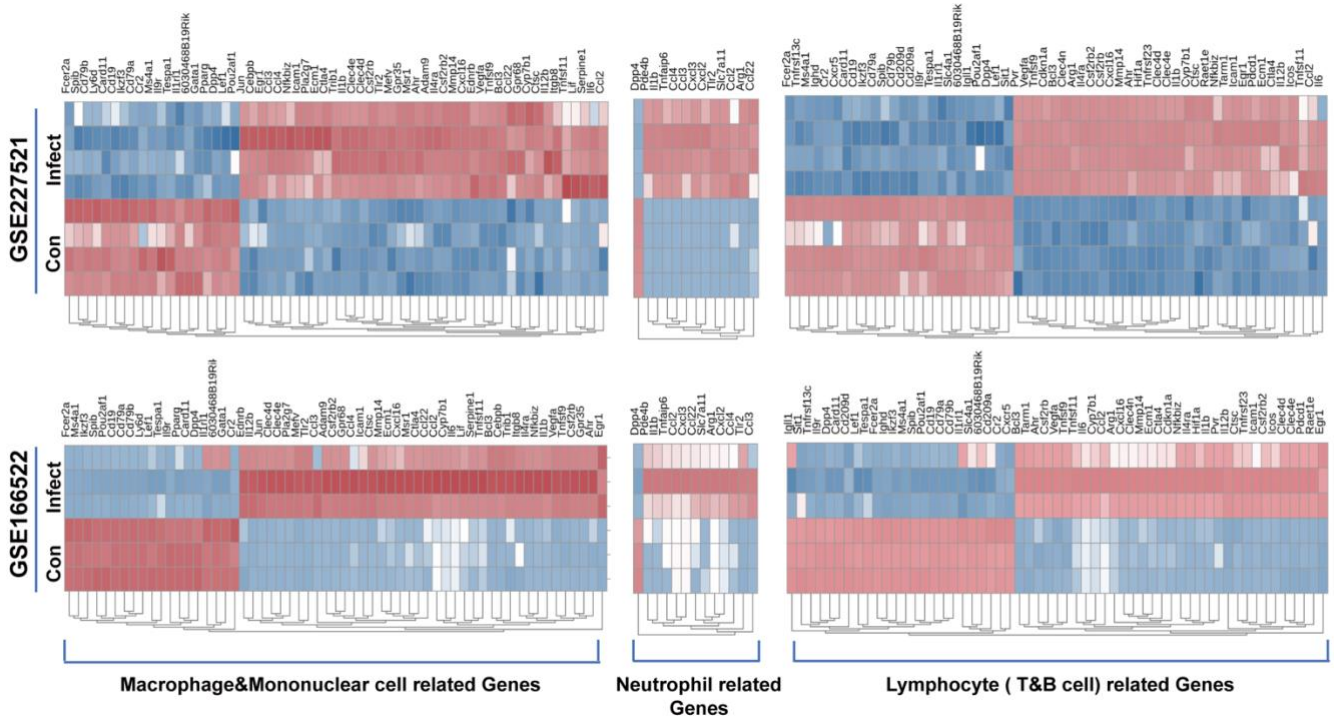

Figure S1. Heatmaps of DEGs related to various immune cell types.

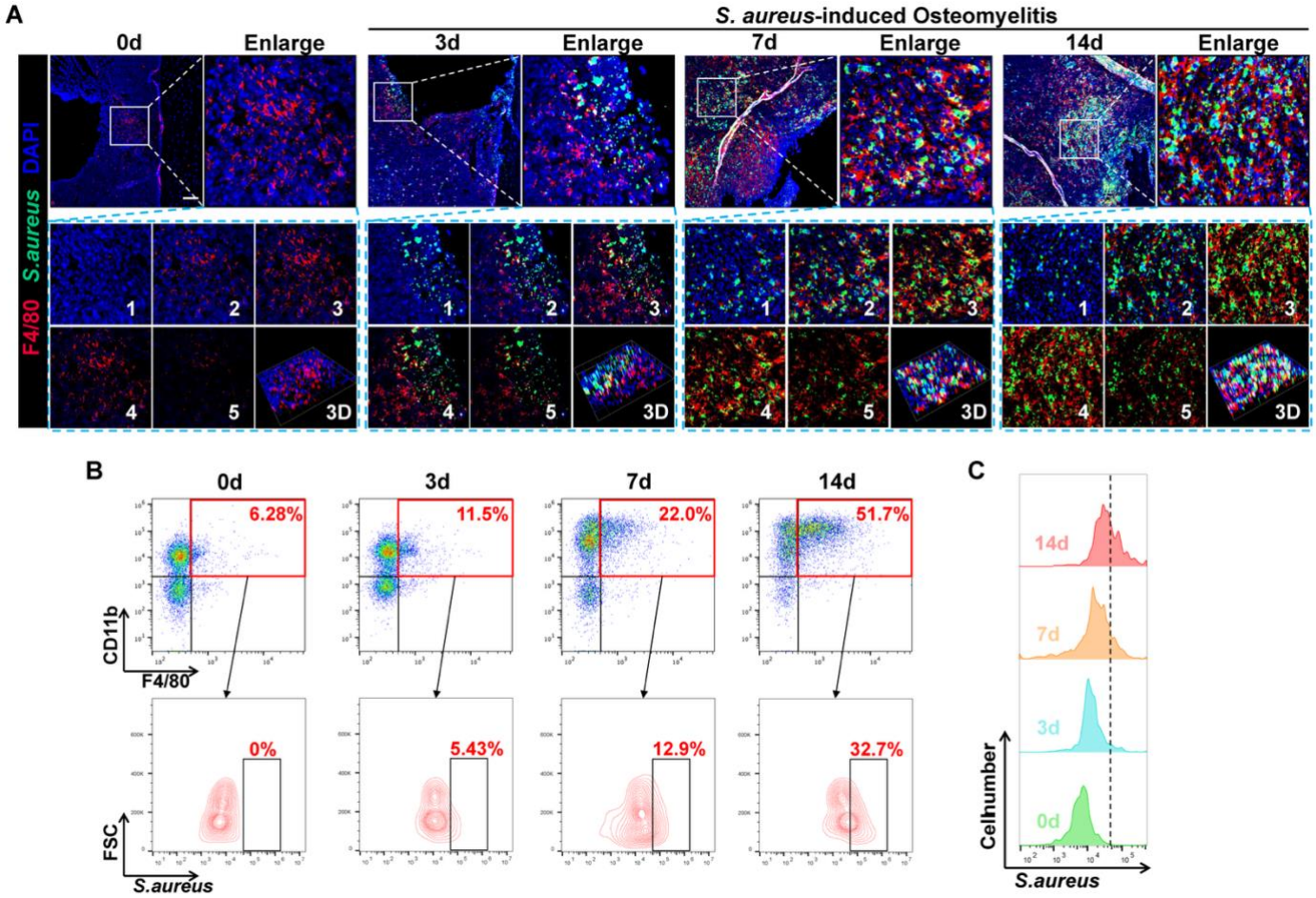

Figure S2. Immunofluorescence staining and flow cytometry show the intracellular *Staphylococcus aureus* (*S. aureus*) in macrophages in *S. aureus*-induced osteomyelitis (SIOM) mice. (A) Representative confocal laser scanning microscopy images and 3D reconstruction of frozen bone tissue sections. Immunofluorescence staining shows *S. aureus* signals (green) enveloped by F4/80$^+$ macrophage membrane signals (red), confirming their intracellular localization. Scale bars, 100 μm. n = 3/group. (B) Representative flow cytometry plots and (C) quantification of the fraction of F4/80$^+$ macrophages with intracellular bacterial residence in the bone lesion. n = 5/group. Source data are provided as a Source Data file.

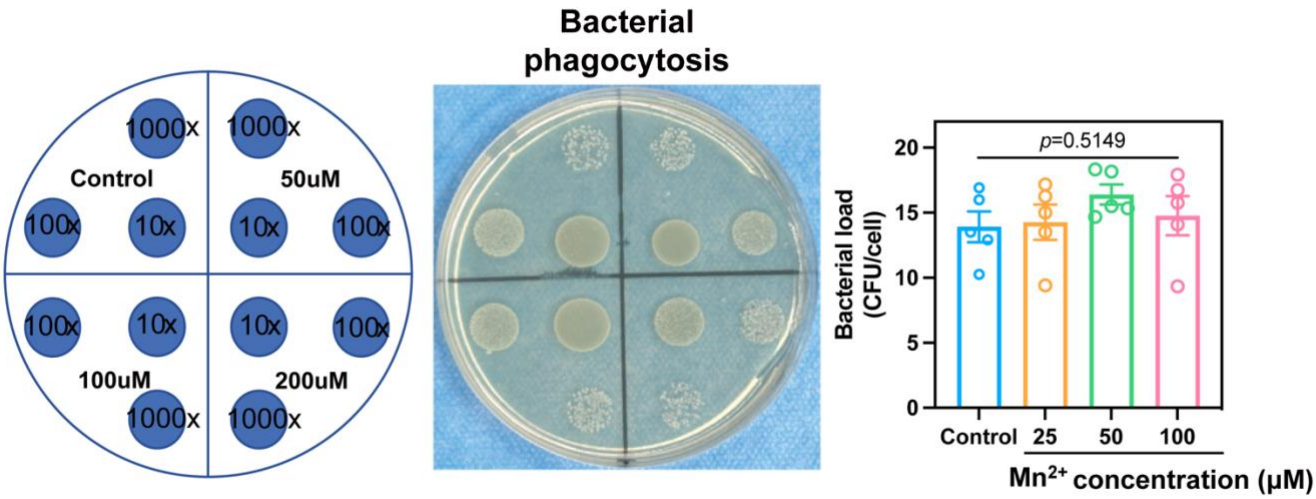

Figure S3. Mn^{2+} treatment exhibits negligible impact on the phagocytic capacity bone marrow-derived macrophages (BMDMs). Representative image and quantitative analysis of phagocytosis activities in *Staphylococcus aureus* (*S. aureus*)-infected BMDMs treated with Mn^{2+} at different concentrations (25, 50, 100 μM). n = 5 biological independent experiments. Data are shown as means ± SEM. Statistical significance was assessed using two-tailed one-way ANOVA with Turkey's post hoc test. Statistical significance is indicated in the figure with corresponding *p* values. Source data are provided as a Source Data file.

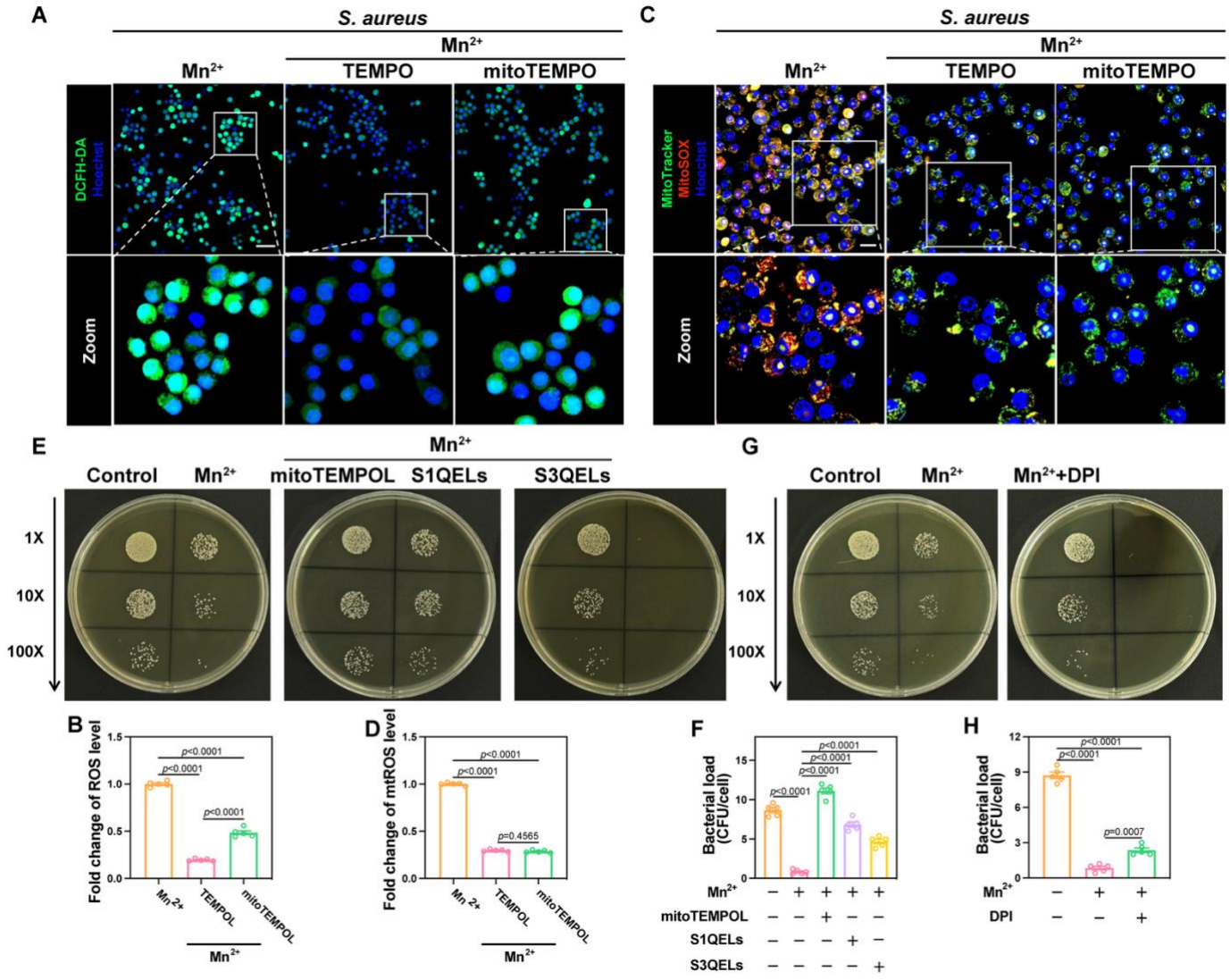

Figure S4. Mn^{2+}-amplified mitochondrial ROS (mtROS) drives the enhanced bactericidal activity of *Staphylococcus aureus* (*S. aureus*)-infected macrophages. (A, C) Representative fluorescence images and (B, D) quantification of total ROS (DCFH-DA) and mtROS (MitoSOX) levels in Mn^{2+}-treated macrophages. General ROS scavenger TEMPOL and mitochondria-targeted scavenger mitoTEMPOL were used to verify the specificity of mtROS scavenging. Scale bars, 50 μm (A) and 20 μm (C). n = 3/group. (E, F) Quantification of intracellular *S. aureus* survival in Mn^{2+}-treated macrophages following mtROS scavenging with mitoTEMPOL or inhibition of mtROS generation at ETC sites using S1QELs and S3QELs. n = 5 biological independent experiments. (G, H) Assessment of intracellular bacterial clearance in Mn^{2+}-treated macrophages in the presence or absence of the NOX inhibitor DPI. n = 5 biological independent experiments. Data are shown as means ± SEM. Statistical significance was assessed using two-tailed one-way ANOVA with Turkey's post hoc test. Statistical significance is indicated in the figure with corresponding *p* values. Source data are provided as a Source Data file.

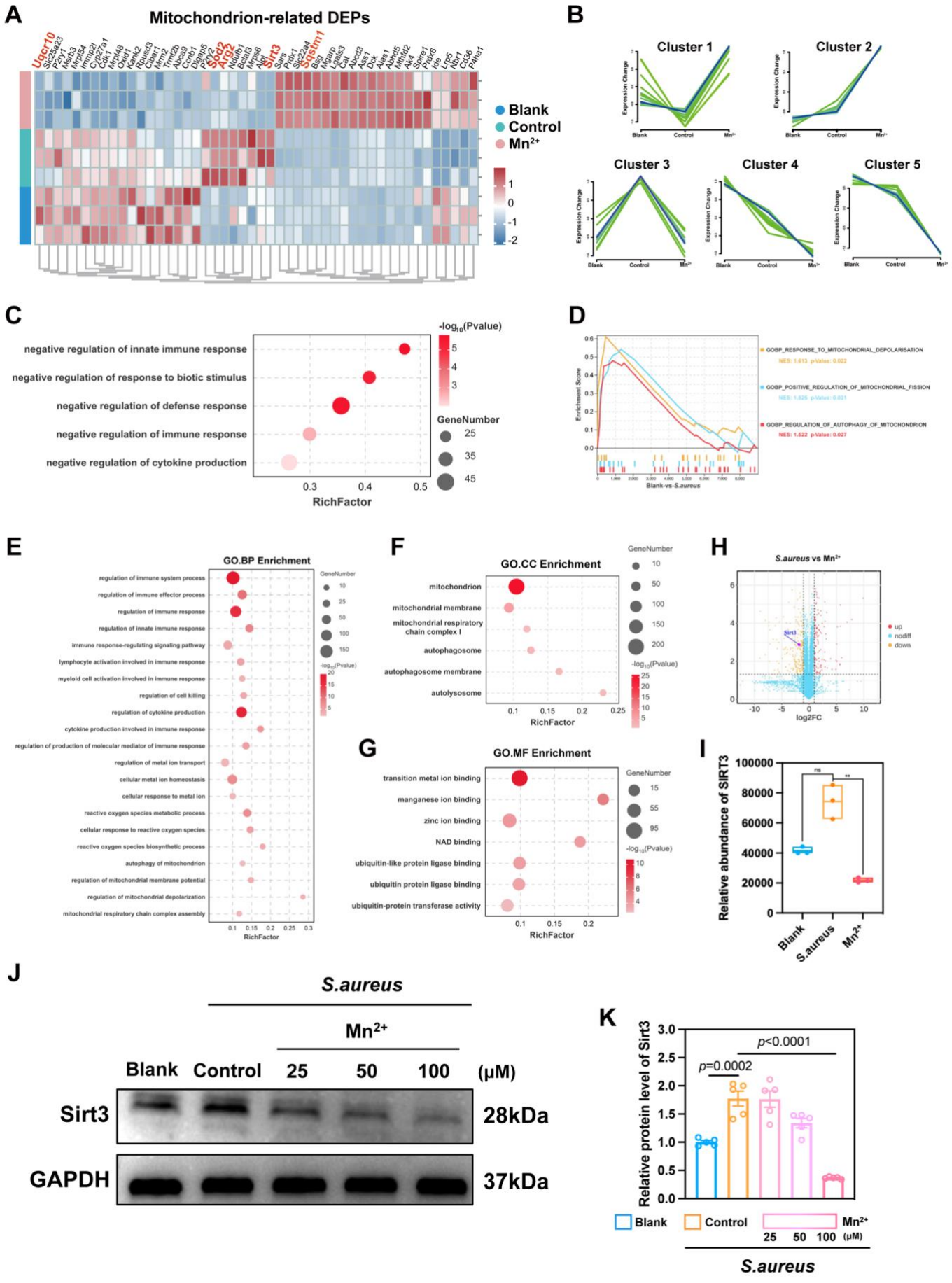

Figure S5. Integrated proteomic profiling and functional validation identify mitochondrial Sirt3 as a key target of Mn^{2+}. (A) Heatmaps of mitochondrion-related differentially expressed proteins (DEPs) in uninfected,

Staphylococcus aureus (*S. aureus*)-infected and Mn^{2+}-treated *S. aureus*-infected bone marrow-derived macrophages (BMDMs). (B) Mfuzz cluster analysis in mitochondrion-related DEPs from BMDMs in indicated groups. (C, D) Bioinformatic analysis in proteomics of uninfected BMDMs (Blank) and *S. aureus*-infected BMDMs (Control). GO biological process enrichment (C) of DEPs and Gene Set Enrichment Analysis (GSEA) (D) between the blank group and the control group exhibit the immunosuppressive state and upregulation of mitophagy in *S. aureus*-infected BMDMs. (E-G) GO functional enrichment analysis of DEPs between the control and the Mn^{2+} group, including biological processes (E), cellular components (F), and molecular functions (G). (H) Volcano plot of DEPs between the control and Mn^{2+} group. (I) Relative abundance of Sirt3 among the indicated three groups. (J, K) Western blot detection of Sirt3 expression levels in uninfected BMDMs, *S. aureus*-infected BMDMs, and *S. aureus*-infected BMDMs treated with Mn^{2+} at different concentrations (25, 50, 100 μM). n = 5 biological independent experiments. Data are shown as means ± SEM. Statistical significance was assessed using two-tailed one-way ANOVA with Turkey's post hoc test. Statistical significance is indicated in the figure with corresponding *p* values. Source data and uncropped Western blot images are provided as a Source Data file.

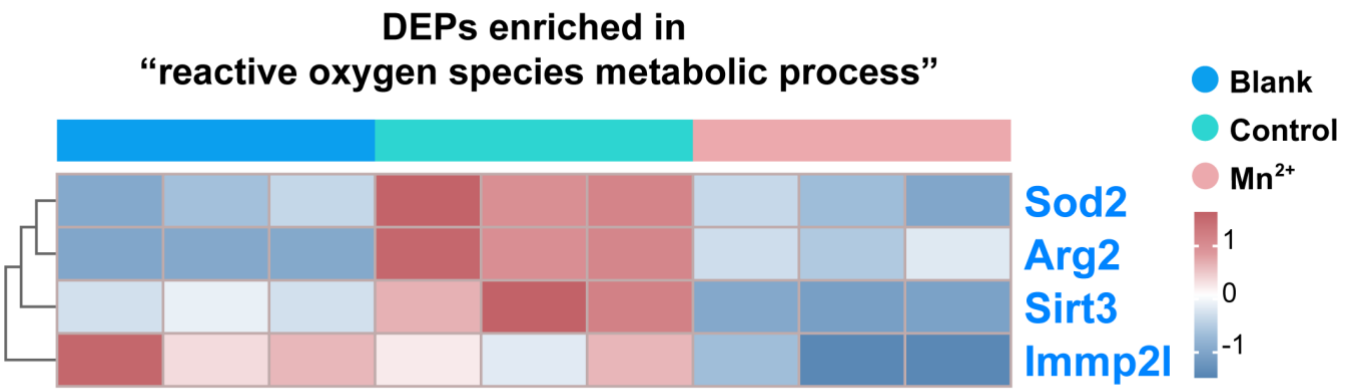

Figure S6. Heatmap of DEPs enriched in the “reactive oxygen species metabolic process” category. Source data are provided as a Source Data file.

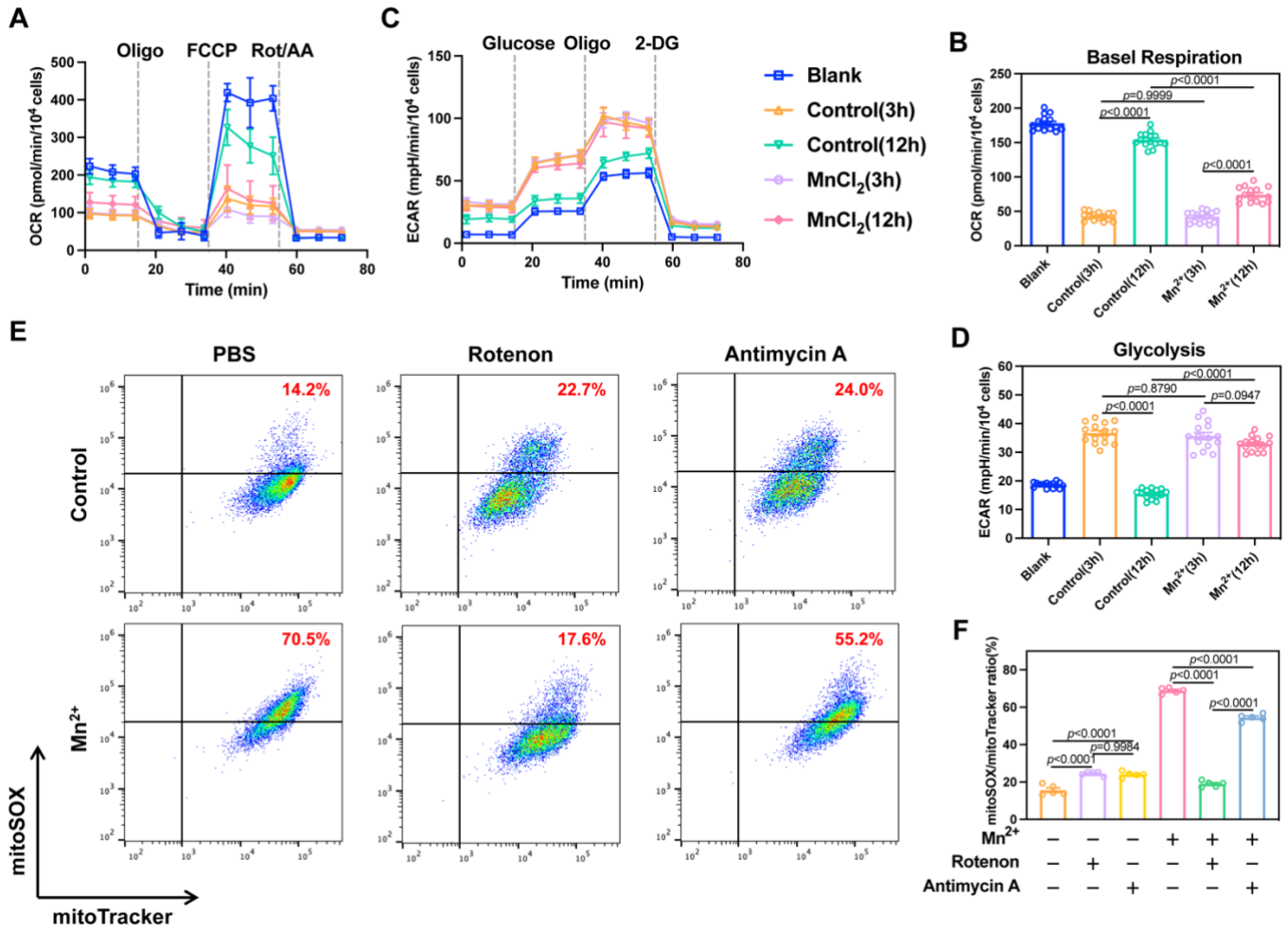

Figure S7. Mn^{2+} addition increases glycolysis in *Staphylococcus aureus* (*S. aureus*)-infected macrophages, and sustains the RET-mediated ROS generation. (A-D) Seahorse extracellular flux analysis and quantitative analysis of OCR and basal respiration (A, B) and ECAR and glycolytic activity (C, D) in macrophages under indicated treatments. n = 13/group at least. (E, F) Flow cytometry analysis and quantitative analysis of mitochondrial ROS (mtROS) in macrophages with indicated treatment. n = 5/group. Data are shown as means ± SEM. Statistical significance was assessed using two-tailed one-way ANOVA with Turkey's post hoc test. Statistical significance is indicated in the figure with corresponding *p* values. Source data are provided as a Source Data file.

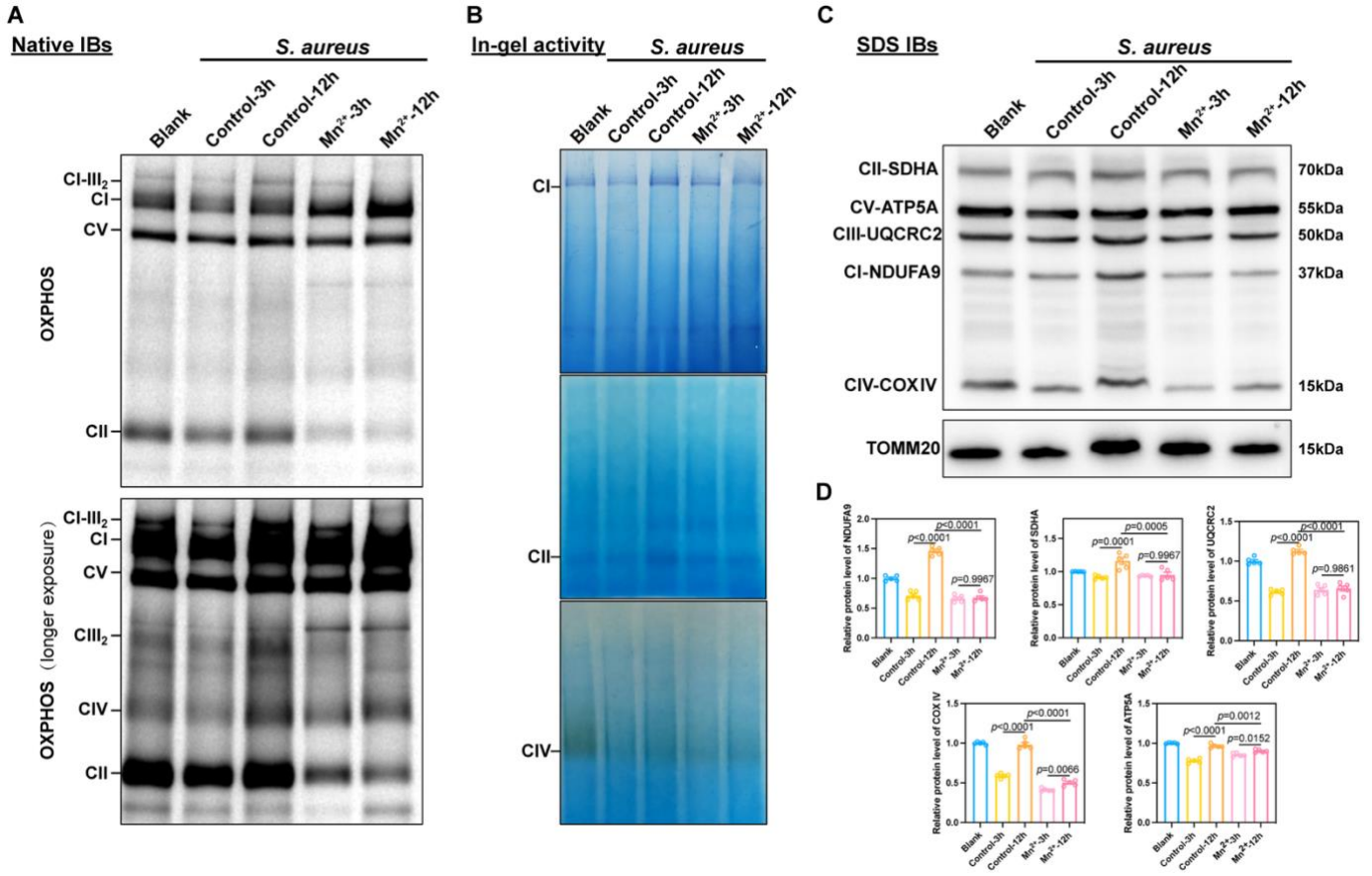

Figure S8. Mn^{2+} treatment suppresses electron transport chain (ETC) complex assembly and activity in *Staphylococcus aureus* (*S. aureus*)-infected bone marrow-derived macrophages (BMDMs). (A) Blue native PAGE (BN-PAGE) analysis of OXPHOS complexes and supercomplexes in macrophages under the indicated treatments (Blank, Control-3h, Control-12h, Mn^{2+}-3h, Mn^{2+}-12h) following *S. aureus* stimulation. (B) In-gel activity assays of mitochondrial respiratory chain complexes (CI, CII, CIV) in macrophages under the indicated treatments following *S. aureus* stimulation. (C, D) SDS IBs and quantitative analysis of representative electron transport chain (ETC) subunits, in macrophages under the indicated treatments following *S. aureus* stimulation. n = 5 biological independent experiments. Data are shown as means ± SEM. Statistical significance was assessed using two-tailed one-way ANOVA with Turkey's post hoc test. Statistical significance is indicated in the figure with corresponding *p* values. Source data and uncropped immunoblot images are provided as a Source Data file.

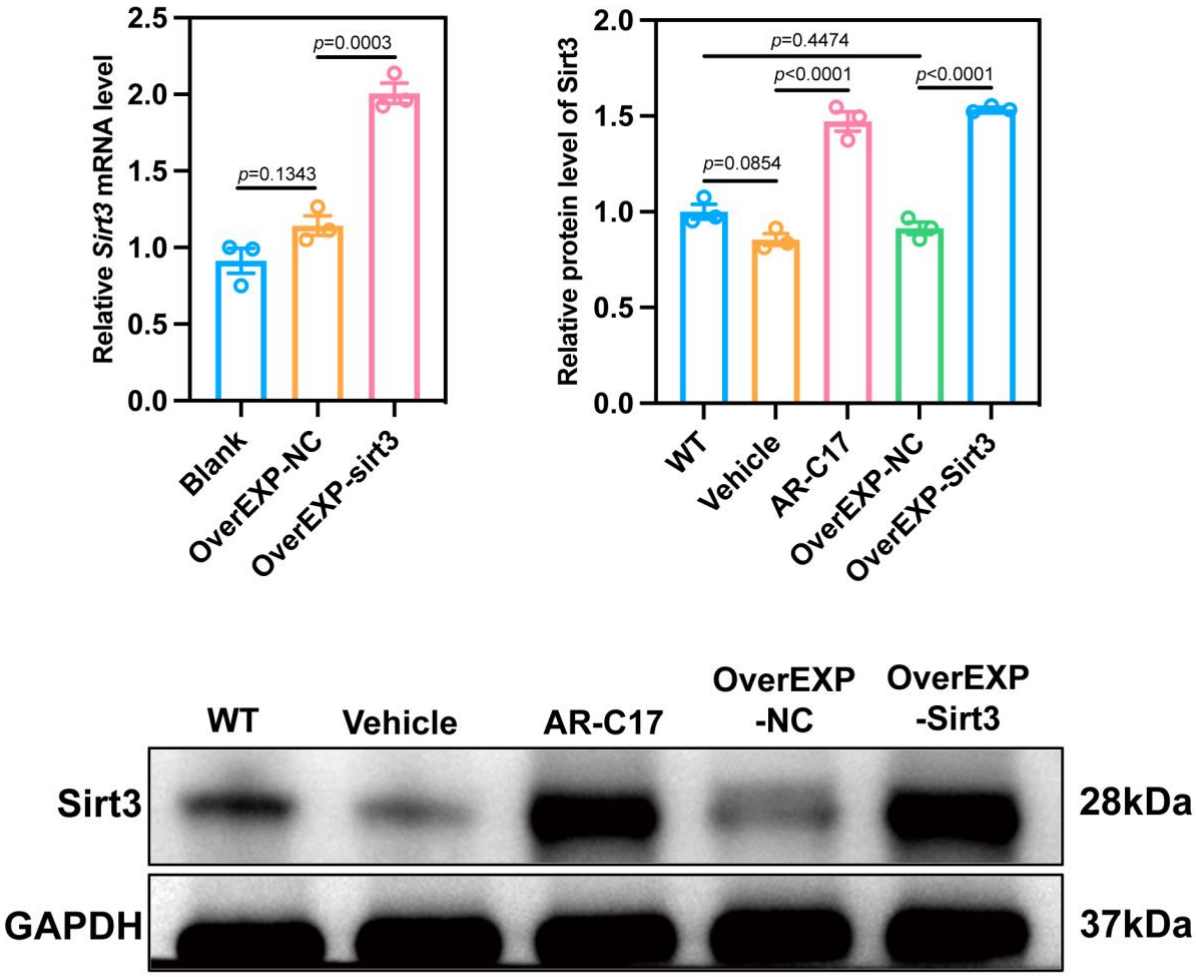

Figure S9. Validation of Sirt3 overexpression in *Staphylococcus aureus* (*S. aureus*)-infected bone marrow-derived macrophages (BMDMs). Measurement of the overexpression efficiency via Sirt3 activator AR-C17 (15μM) and transfection of mouse Sirt3 overexpression plasmid by qPCR and Western blot. n = 3 biological independent experiments. Data are shown as means ± SEM. Statistical significance was assessed using two-tailed one-way ANOVA with Turkey's post hoc test. Statistical significance is indicated in the figure with corresponding *p* values. Source data and uncropped Western blot images are provided as a Source Data file.

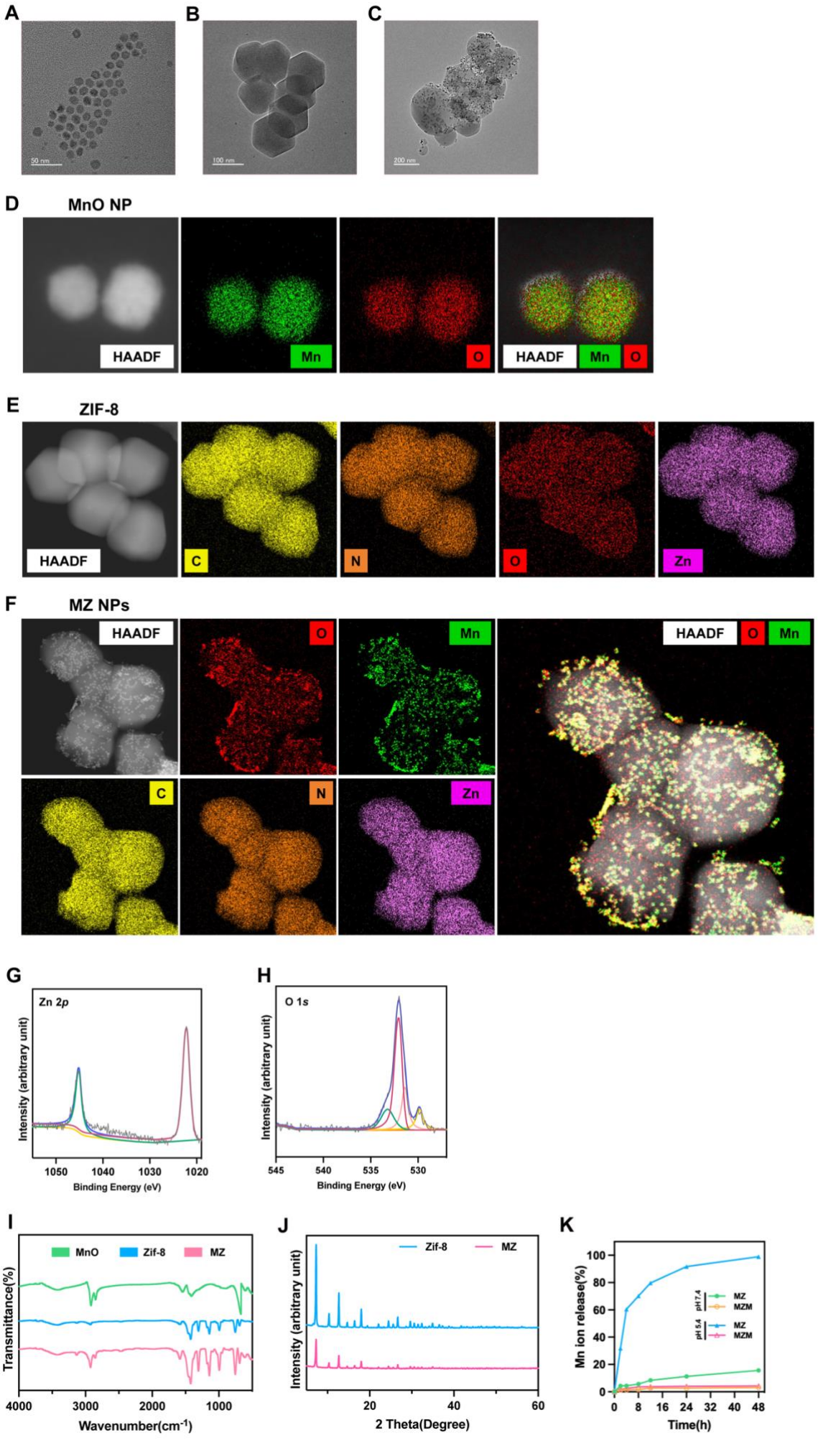
A
B
C
50 nm
100 nm
200 nm
D
MnO NP
HAADF
Mn
O
HAADF
Mn
O
E
ZIF-8
HAADF
C
N
O
Zn
F
MZ NPs
HAADF
O
Mn
HAADF
O
Mn
C
N
Zn
G
Zn 2p
Intensity (arbitrary unit)
1050
1040
1030
1020
Binding Energy (eV)
H
O 1s
Intensity (arbitrary unit)
545
540
535
530
Binding Energy (eV)
I
MnO
Zif-8
MZ
Transmittance(%)
4000
3000
2000
1000
Wavenumber(cm-1)
J
Zif-8
MZ
Intensity (arbitrary unit)
20
40
60
2 Theta(Degree)
K
Mn ion release(%)
100
80
60
40
20
0
pH7.4
MZ
MZM
pH5.4
MZ
MZM
0
8
16
24
32
40
48
Time(h)

Figure S10. Characterization of synthesized nanomaterials (MnO NPs, ZIF-8, and MZ NPs). (A-F) Representative transmission electron microscopy (TEM) images of MnO NPs, Scale bars, 50 nm (A), ZIF-8 NPs, Scale bars, 100 nm (B), and MZ NPs, Scale bars, 200 nm (C), high-angle annular dark-field scanning transmission electron microscopy (HAADF-STEM) images and EDS elemental mapping of MnO NPs (D), ZIF-8 NPs (E), and MZ NPs (F). (G, H) High-resolution Zn 2p (G) and O 1s (H) XPS spectrum of MZ NPs. (I) FT-IR spectra of MnO NPs, ZIF-8, and MZ NPs. (J) XRD patterns of ZIF-8 and MZ NPs. (K) Mn^{2+} release profiles of MZ NPs and macrophage membrane-coated MnO-loaded ZIF-8 (MZM) nano-system under different pH conditions (pH = 5.4 and 7.4). n = 3/group. Source data are provided as a Source Data file.

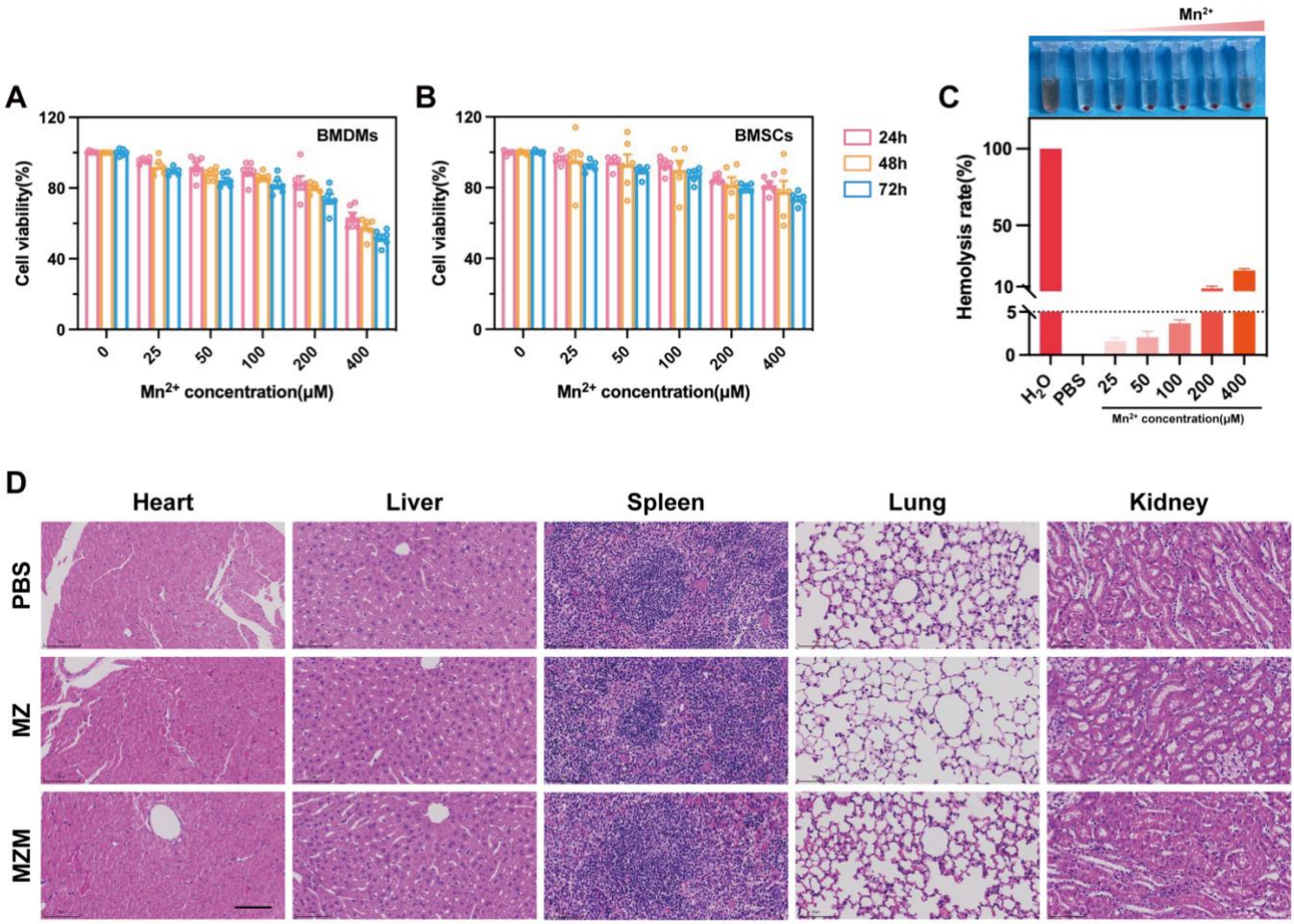

Figure S11. Biocompatibility and safety of synthesized macrophage membrane-coated MnO-loaded ZIF-8 (MZM) nano-system. (A, B) CCK-8 assay shows the cell viabilities of BMDMs and bone marrow mesenchymal stem cells (BMSCs) under different concentrations (25, 50, 100, 200, 400 μM) of Mn^{2+} in MZM. n = 5 biological independent experiments. (C) Hemolytic assay shows the hemocompatibility of MZM at different concentrations (25, 50, 100, 200, 400 μM) on red blood cells. n = 3 biological independent experiments. (D) Representative hematoxylin and eosin (H&E) staining images of major organs from the mice treated with PBS, MZ and MZM at day 21 post-treatment. Scale bars, 50 μm. n = 5/group. Data are shown as means ± SEM. Source data are provided as a Source Data file.

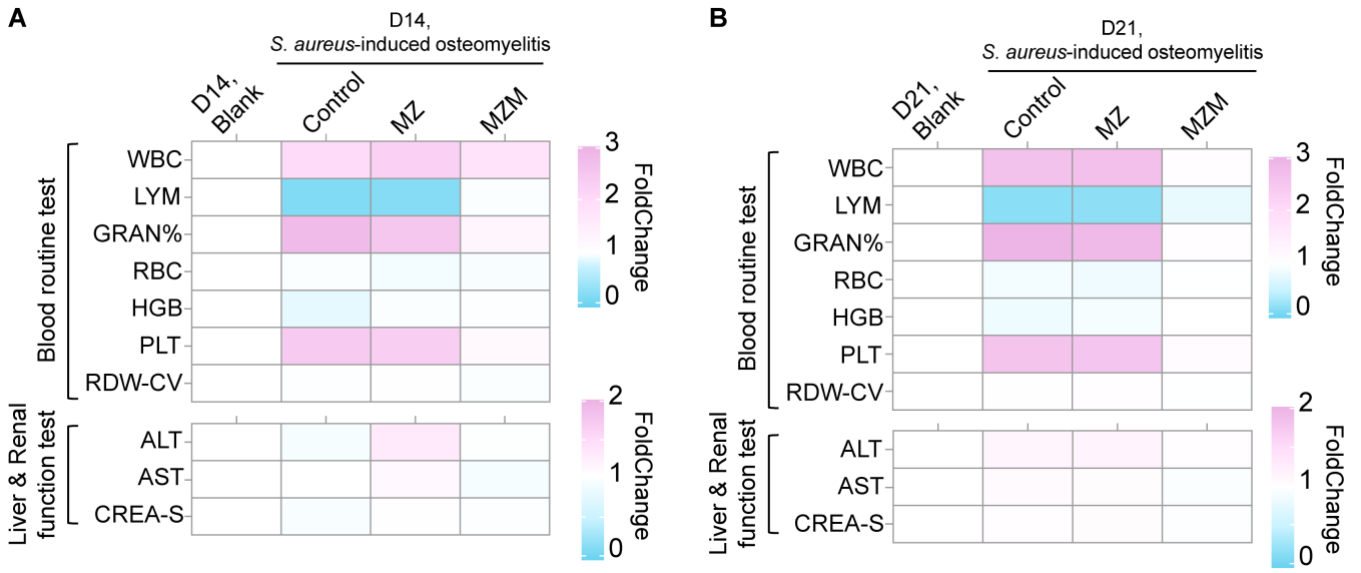

Figure S12. Blood routine test (BRT) and serum biochemistry analyses. n = 5/group. Source data are provided as a Source Data file.

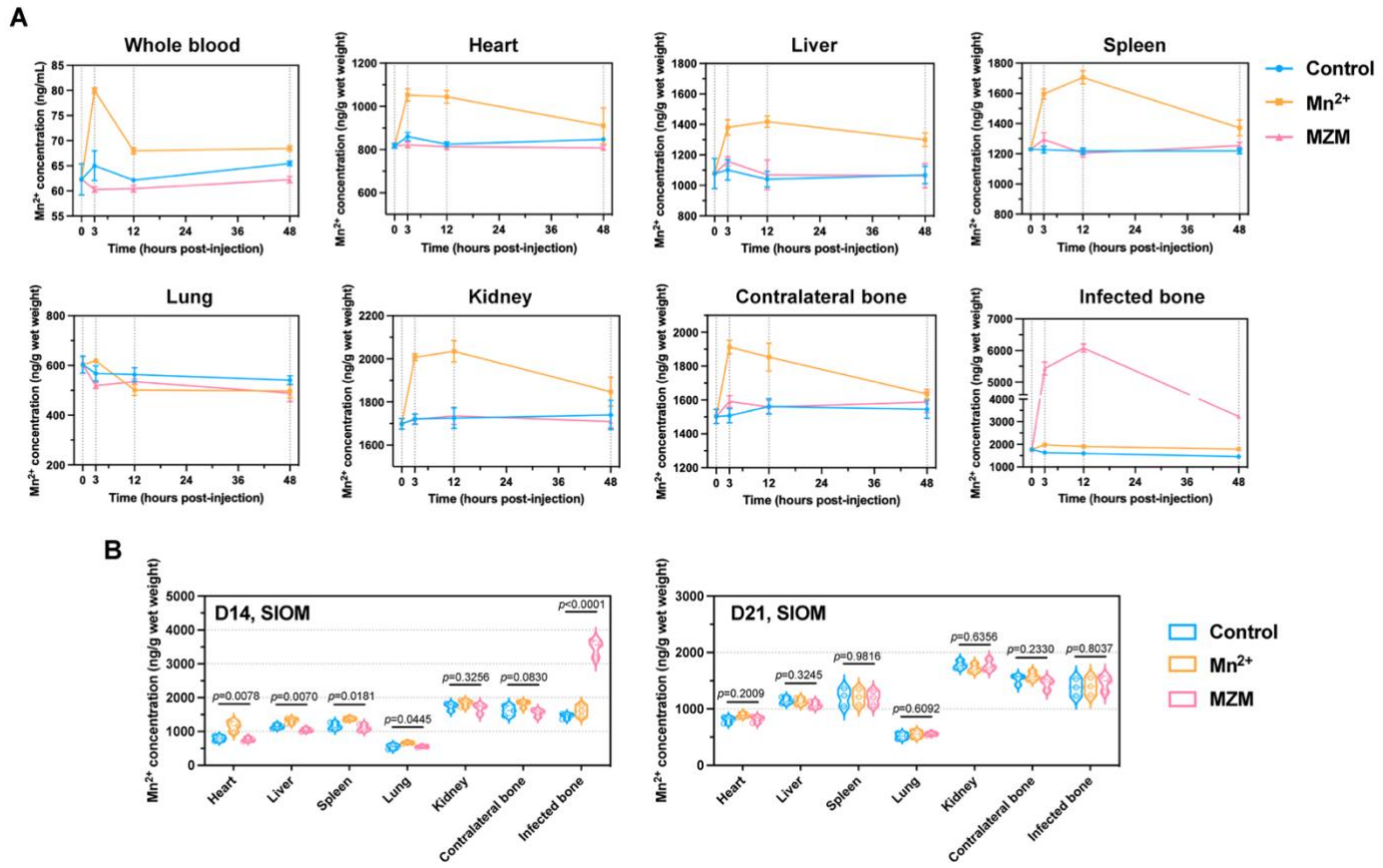

Figure S13. Mn levels within 48 h (short-term) and at day 14 and day 21 (mid-long term) after macrophage membrane-coated MnO-loaded ZIF-8 (MZM) nano-system administration. (A) Quantitative analysis of Mn concentrations in whole blood, heart, liver, spleen, lung, kidney, contralateral bone, and infected bone at different time points (0, 3, 12, and 48 h) after tail vein injection of Mn^{2+}, or MZM. (B) Violin plots showing the distribution of Mn concentrations in major organs, contralateral bone, and infected bone at day14 post-injection (continuous dosing regimen of every two days), and at day 21 (7 days after treatment cessation). n = 3/group. Data are shown as means ± SEM. Statistical significance was assessed using two-tailed one-way ANOVA test. Statistical significance is indicated in the figure with corresponding *p* values. Source data are provided as a Source Data file.

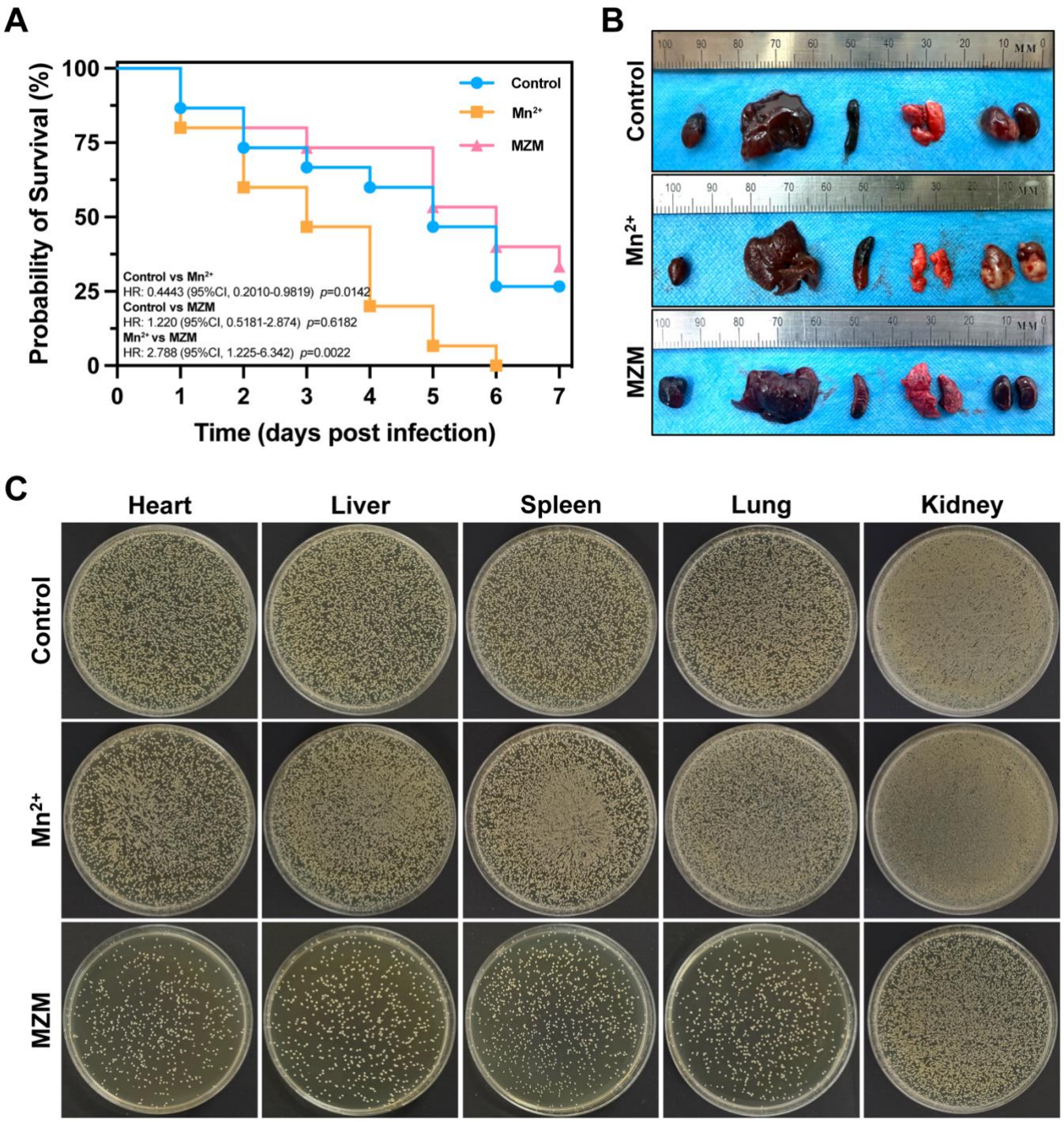

Figure S14. The macrophage membrane-coated MnO-loaded ZIF-8 (MZM) nano-system does not cause exacerbation of the outcomes in systemic *Staphylococcus aureus* (*S. aureus*) infection model. (A) Survival curves of systemically infected mice with *S. aureus* and treated with Mn^{2+}, or MZM, monitored post-infection. n (control) = 11, n (Mn^{2+}) = 15, n (MZM) = 10. (B) Representative images of major organs harvested from systemically infected mice with *S. aureus* treated with Mn^{2+}, or MZM. n = 3/group. (C) Representative agar plates displaying bacterial burden in major organs of systemically infected mice with *S. aureus* treated with Mn^{2+}, or MZM. n = 3/group. Statistical significance was assessed using Log-rank (Mantel-Cox) test. Statistical significance is indicated in the figure with corresponding *p* values. Source data are provided as a Source Data file.

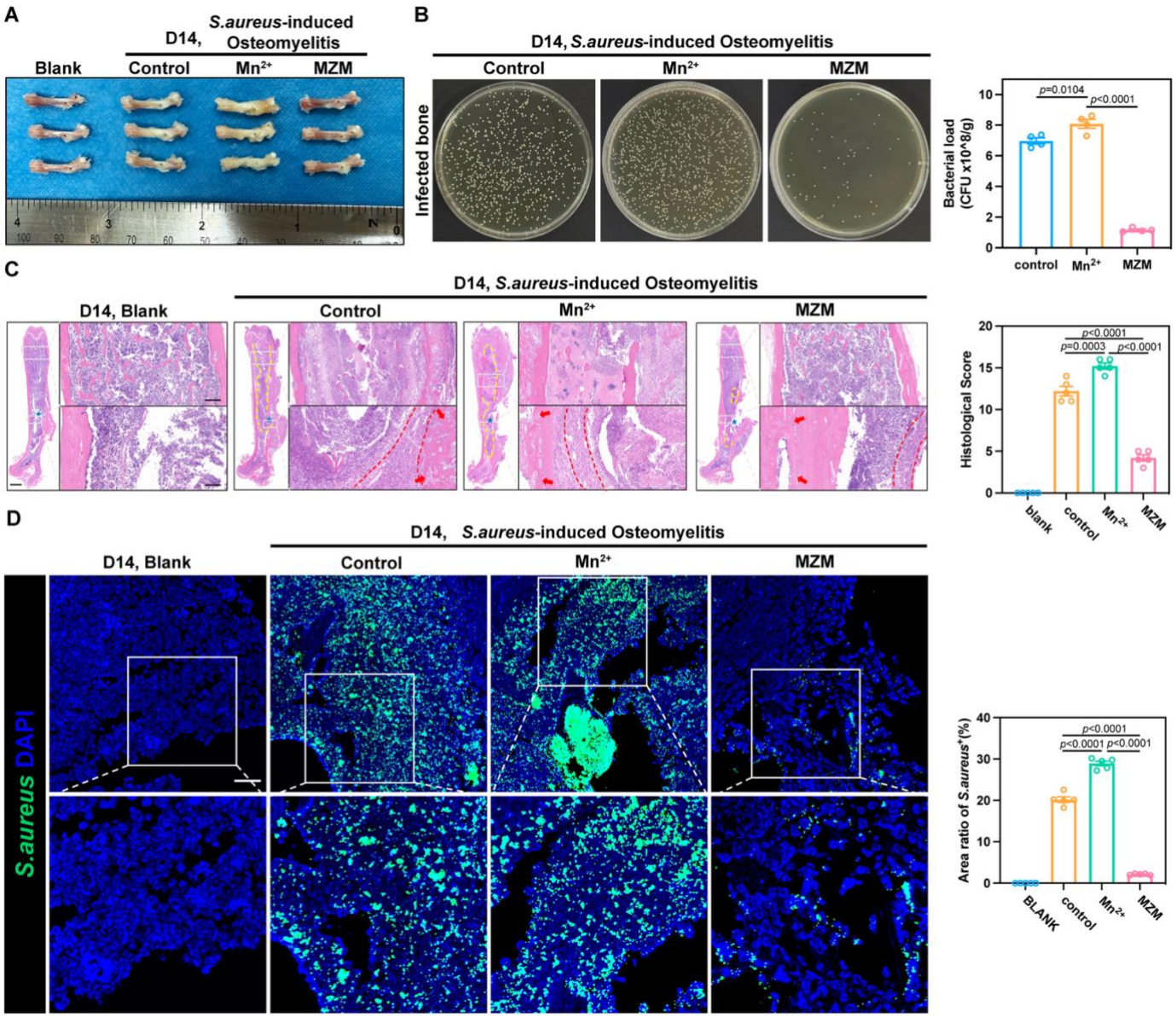

Figure S15. The macrophage membrane-coated MnO-loaded ZIF-8 (MZM) nano-system treatment improves infection control, whereas free Mn^{2+} tends to aggravate local infection severity in *Staphylococcus aureus*-induced osteomyelitis (SIOM) mice. (A) Representative gross images of femurs from SIOM mice with indicated treatment at day 14 post-surgery. n=3/group. (B) Representative agar plates and quantitative analysis of bacterial burden in infected femurs from SIOM mice with indicated treatment at day 14 post-infection. n = 5/group. (C) Representative hematoxylin and eosin (H&E) staining images and histological score of femurs from SIOM mice with indicated treatment at day 14 post-surgery. Scale bars, 1 mm (overview), 250 μm (mid magnification), and 100 μm (high magnification). n = 5/group. (D) Representative fluorescence images and quantitative analysis of the area ratio of *S. aureus*$^+$ in infected femurs from SIOM mice with indicated treatment at day 14 post-surgery. Scale bars, 50 μm. n = 5/group. Data are shown as means ± SEM. Statistical significance was assessed using two-tailed one-way ANOVA with Turkey's post hoc test. Statistical significance is indicated in the figure with corresponding *p* values. Source data are provided as a Source Data file.

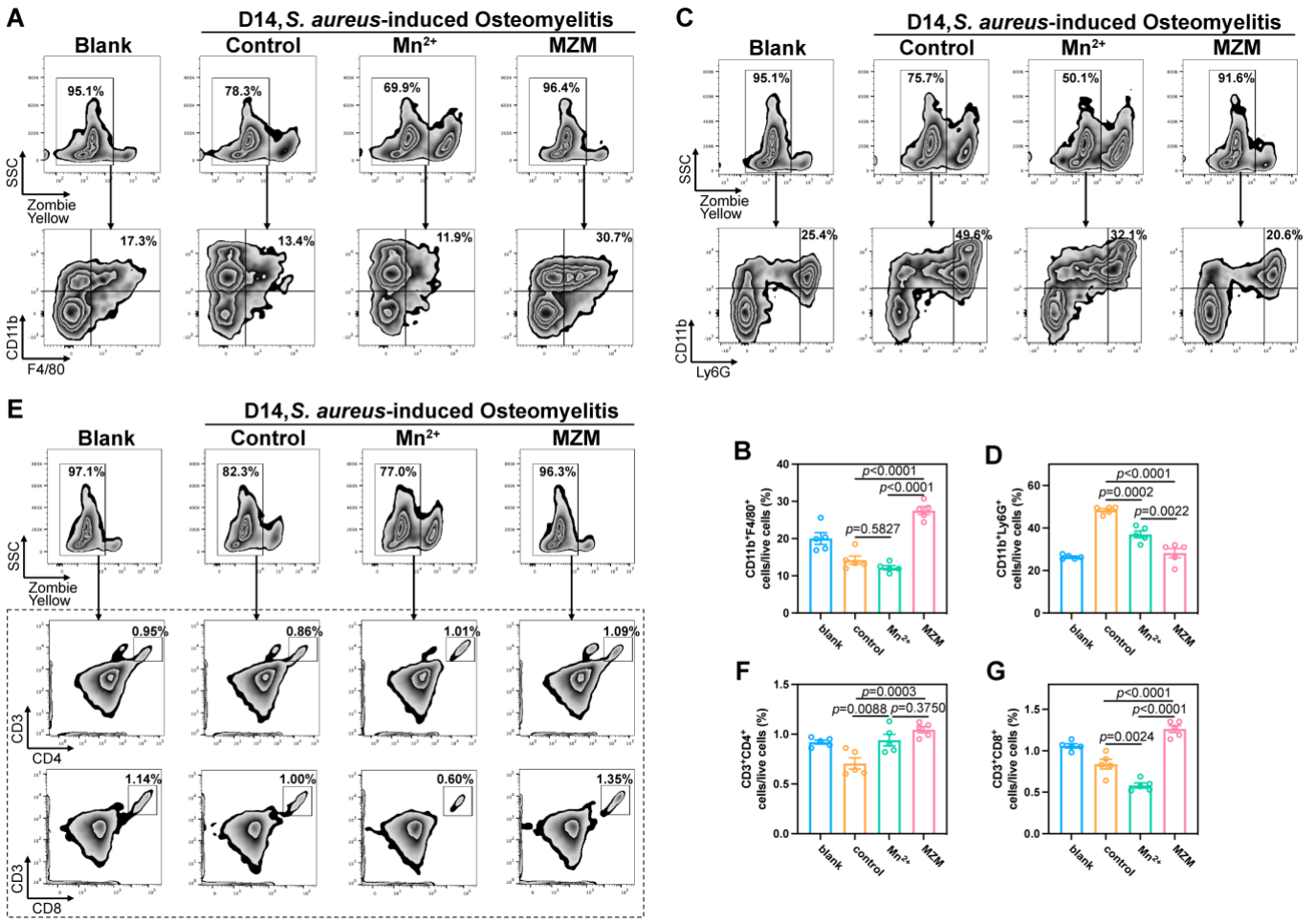

Figure S16. The macrophage membrane-coated MnO-loaded ZIF-8 (MZM) nano-system treatment does not adversely affect the immune response in *Staphylococcus aureus*-induced osteomyelitis (SIOM) mice. (A, B) Representative flow cytometry plots and quantitative analysis of $CD11b^+F4/80^+$ macrophages among live cells from femurs of SIOM mice with indicated treatment at day 14 post-surgery. (C, D) Representative flow cytometry plots and quantitative analysis of $CD11b^+Ly6G^+$ neutrophils among live cells from femurs of SIOM mice with indicated treatment at day 14 post-surgery. (E, F) Representative flow cytometry plots and quantitative analysis of $CD3^+CD4^+$ T cells among live cells. (G) Quantitative analysis of $CD3^+CD8^+$ T cells among live cells. n = 5/group. Data are shown as means ± SEM. Statistical significance was assessed using two-tailed one-way ANOVA with Turkey's post hoc test. Statistical significance is indicated in the figure with corresponding *p* values. Source data are provided as a Source Data file.

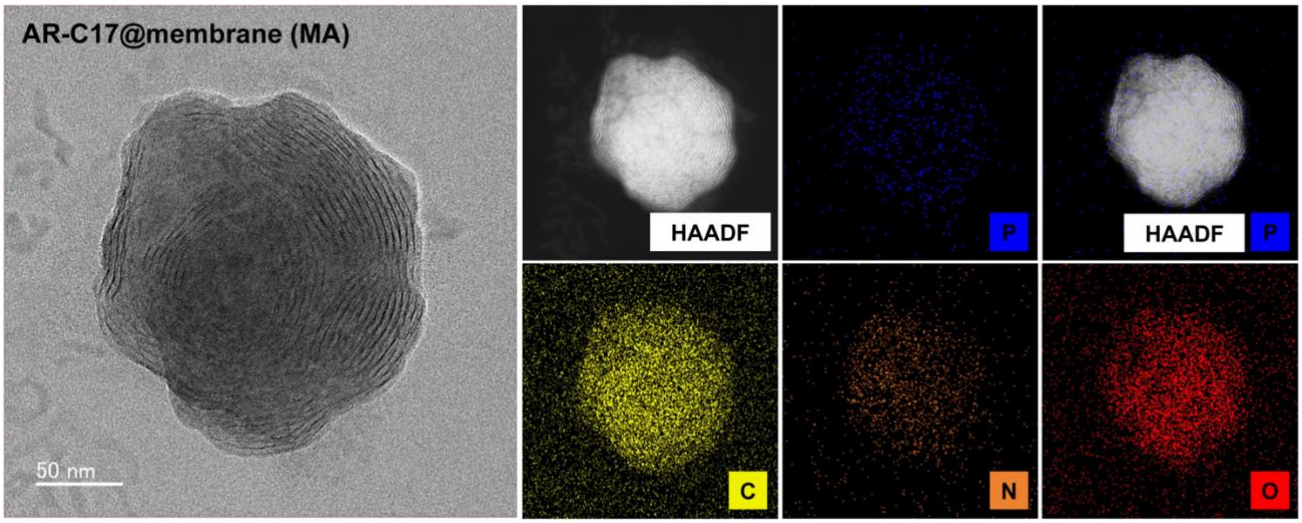

Figure S17. Representative transmission electron microscopy (TEM) images, high-angle annular dark-field scanning transmission electron microscopy (HAADF-STEM) images, and EDS elemental mapping of macrophage membrane-coated AR-C17 (MA).

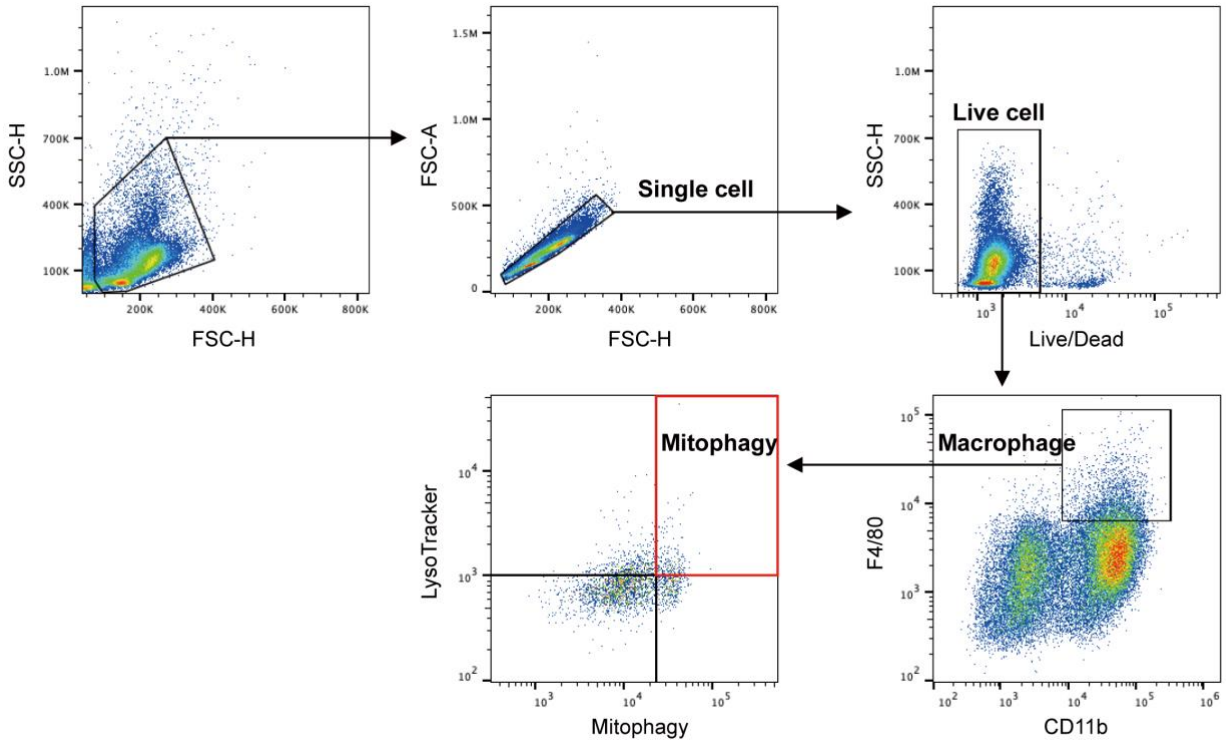

Figure S18. Flow-cytometric gating strategy for measuring mitophagy levels in macrophages.

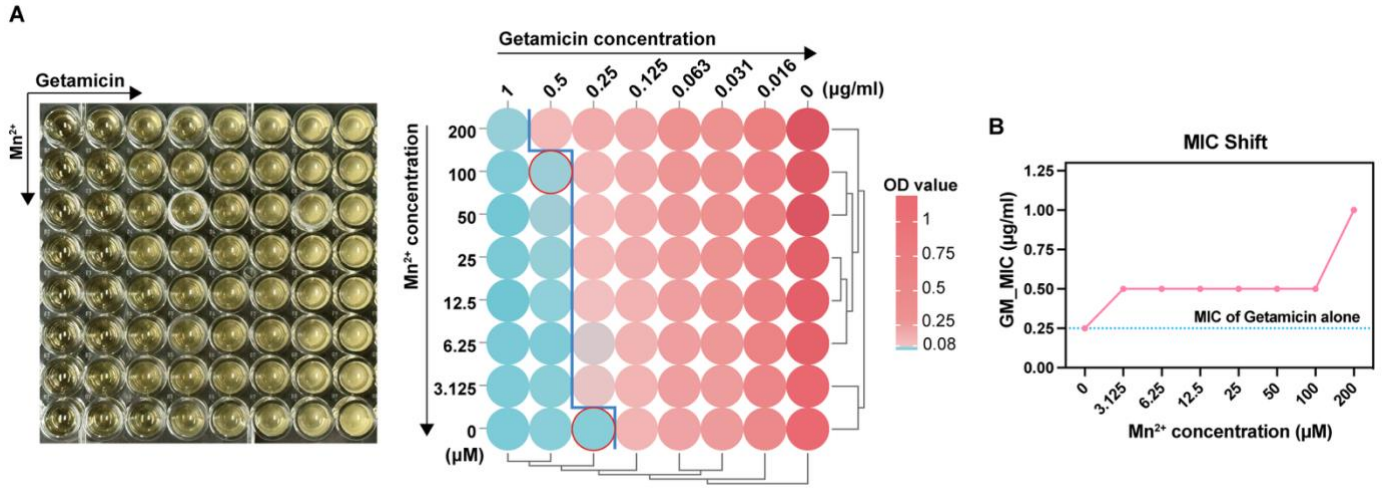

Figure S19. Mn^{2+} does not exhibit synergistic antibacterial effects with gentamicin against *S. aureus* in vitro. (A, B) Bacterial OD measurements and quantitative determination of the minimum inhibitory concentration (MIC) of Gentamicin against *S. aureus* under different concentrations (0, 3.125, 6.25, 12.5, 25, 50, 100, 200 μM) of Mn^{2+} were assessed by a standard checkerboard assay. n = 3 biological independent experiments. Source data are provided as a Source Data file.

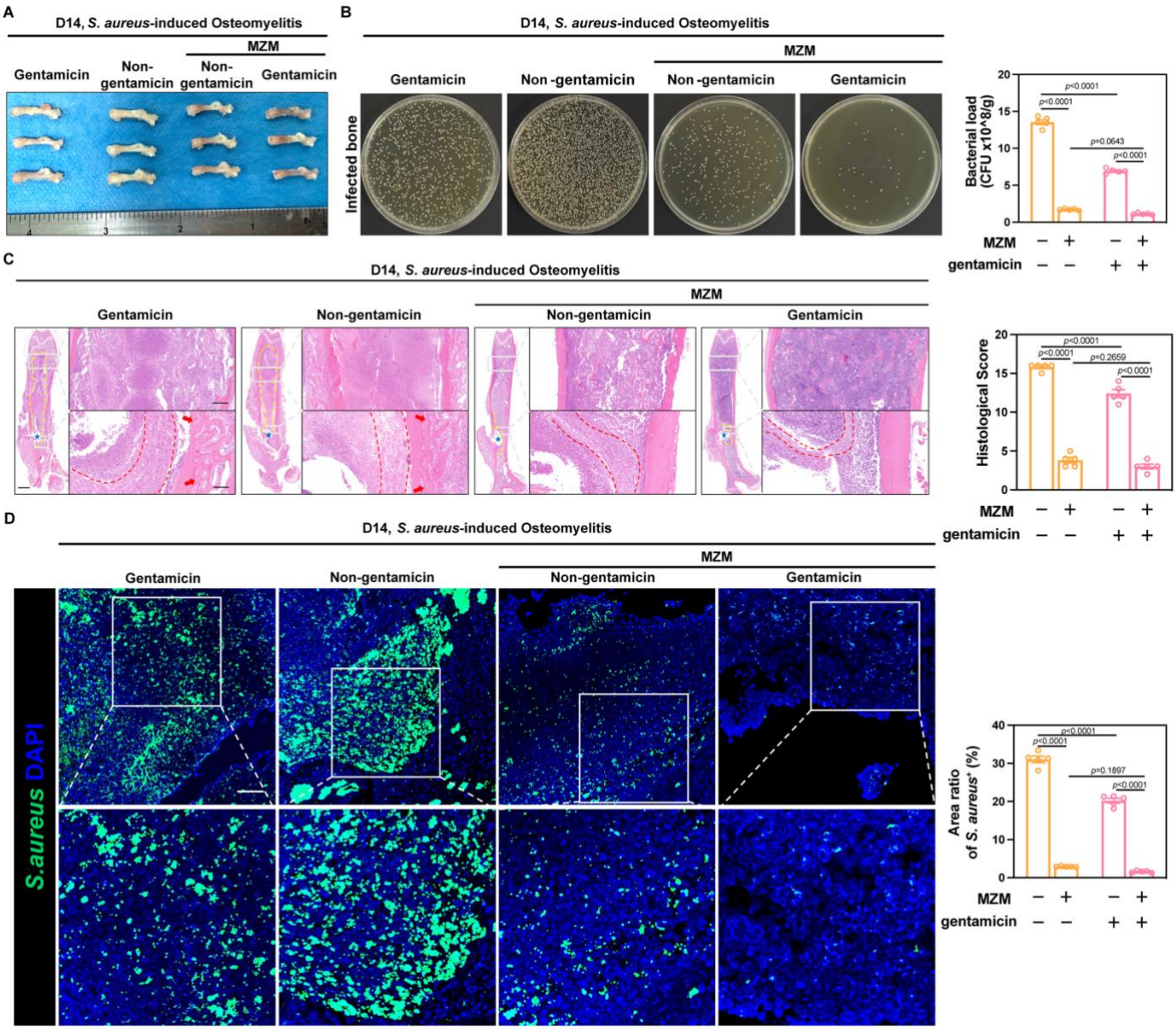

Figure S20. The macrophage membrane-coated MnO-loaded ZIF-8 (MZM) nano-system improves the clinical outcomes predominantly by enhancing macrophage-mediated bactericidal activity. (A) Representative gross images of femurs from *Staphylococcus aureus*-induced osteomyelitis (SIOM) mice with indicated treatment at day 14 post-infection. (B) Representative agar plates and quantitative analysis of bacterial burden in infected femurs from SIOM mice with indicated treatment at day 14 post-infection. (C) Representative hematoxylin and eosin (H&E) staining images and histological score of femurs from SIOM mice with indicated treatment at day 14 post-infection. Scale bars, 1 mm (overview), 250 μm (mid magnification), and 100 μm (high magnification). n = 5/group. (D) Representative fluorescence images and quantitative analysis of the area ratio of *S. aureus* in infected femurs from SIOM mice with indicated treatment at day 14 post-infection. Scale bars, 50 μM. n = 5/group. Data are shown as means ± SEM. Statistical significance was assessed using two-tailed two-way ANOVA with Sidak post hoc test. Statistical significance is indicated in the figure with corresponding *p* values. Source data are provided as a Source Data file.

Table S1. Detail information of GEO datasets

GEO Series	Species/Materials	Group Design	Assay/Platform	Number of Samples	DOI
GSE227521	*Mus musculus*; Bone marrow from *S. aureus* osteomyelitis model	**Day 7 post-operation:** Comparative expression profiling in WT vs ApoE knockout, each with or without S. aureus osteomyelitis	RNA-seq; Illumina HiSeq 4000 (GPL21103)	16	10.3389/fcimb.2023.1187543
GSE166522	*Mus musculus*; Bone marrow from *S. aureus* osteomyelitis model	**Day 3 post-operation:** Control vs Infection **Day 14 post-operation:** Control vs Infection	RNA-seq; Illumina NovaSeq 6000 (GPL24247)	12	10.1128/IAI.00814-20
GSE102444	*Mus musculus*; Alveolar macrophages	**24 h post-*S. aureus* infection:** Alveolar macrophages (i) Uninfected (ii) Infected (iii) Infected + anti-alpha-toxin	Microarray; Affymetrix Mouse Genome 430 2.0 Array (GPL1261)	9	10.1016/j.celrep.2018.02.027

Table S2. Two-way ANOVA analysis of effects of Mn^{2+} and gentamicin on *Staphylococcus aureus*-induced osteomyelitis (SIOM).

Evaluation	Source of Variation	% of total variation	*p* value	F value
Bacterial colonies	Mn^{2+} Factor	77.51	<0.0001	2365
	Gentamicin Factor	12.96	<0.0001	395.3
	Interaction	9.007	<0.0001	274.8
Histological Scoring	Mn^{2+} Factor	93.27	<0.0001	848.1
	Gentamicin Factor	3.593	<0.0001	32.67
	Interaction	1.377	0.0027	12.52
***S. aureus* in bone marrow cavity**	Mn^{2+} Factor	89.53	<0.0001	1905
	Gentamicin Factor	6.032	<0.0001	128.3
	Interaction	3.688	<0.0001	78.46

Uncropped images

Figure S5

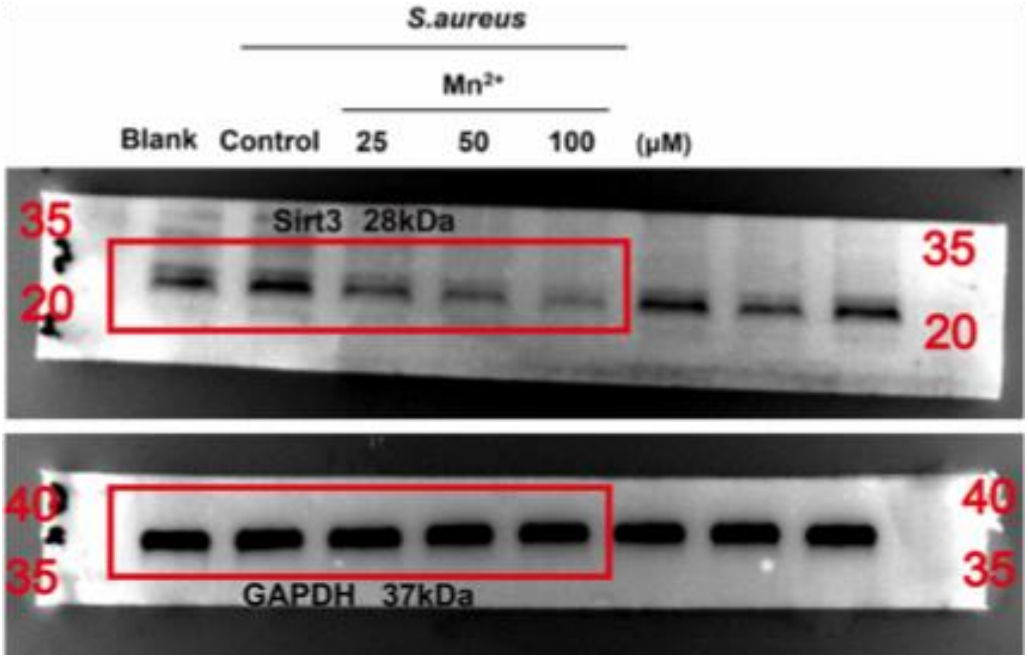

Uncropped images

Figure S8A

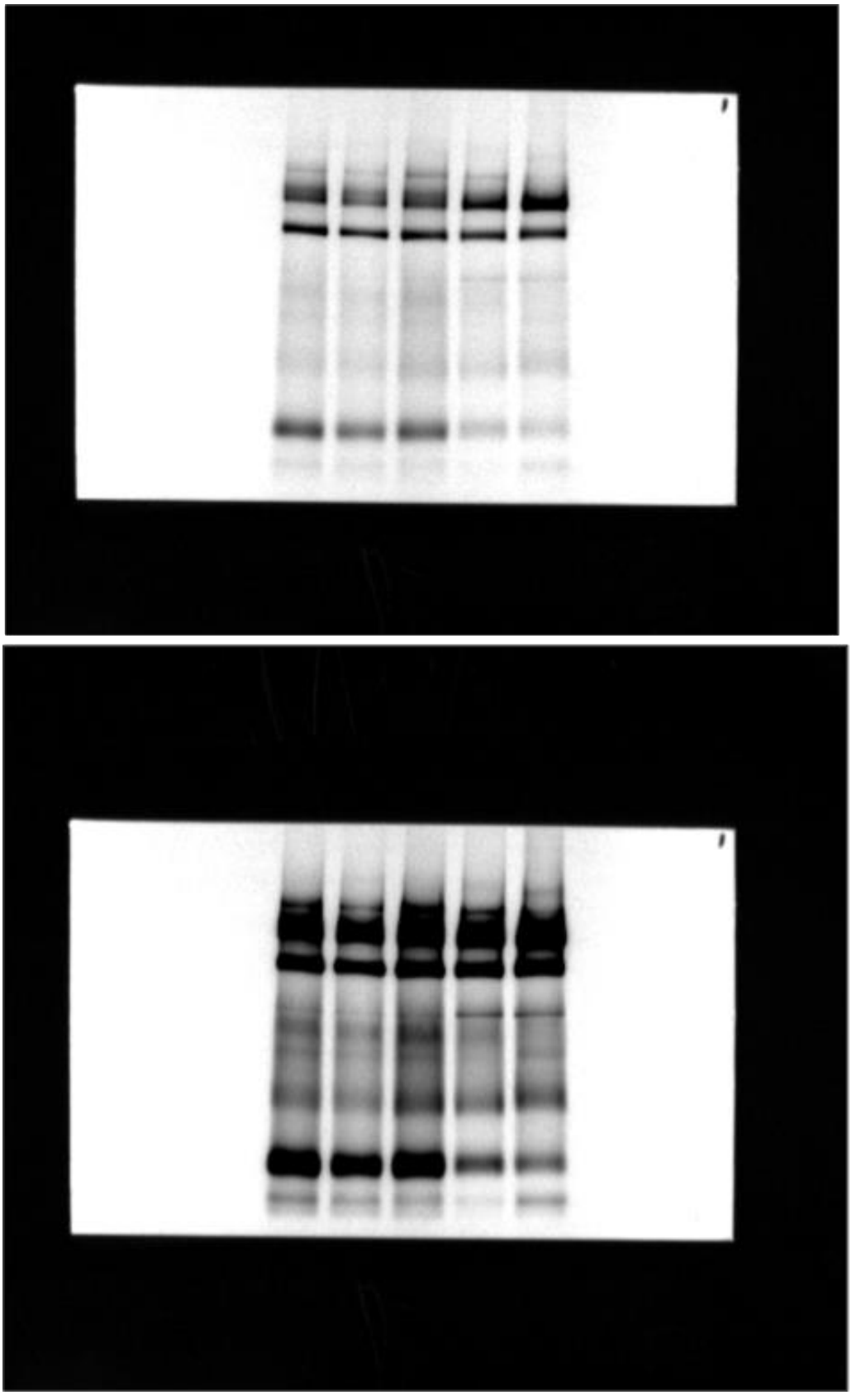

Uncropped images

Figure S8B

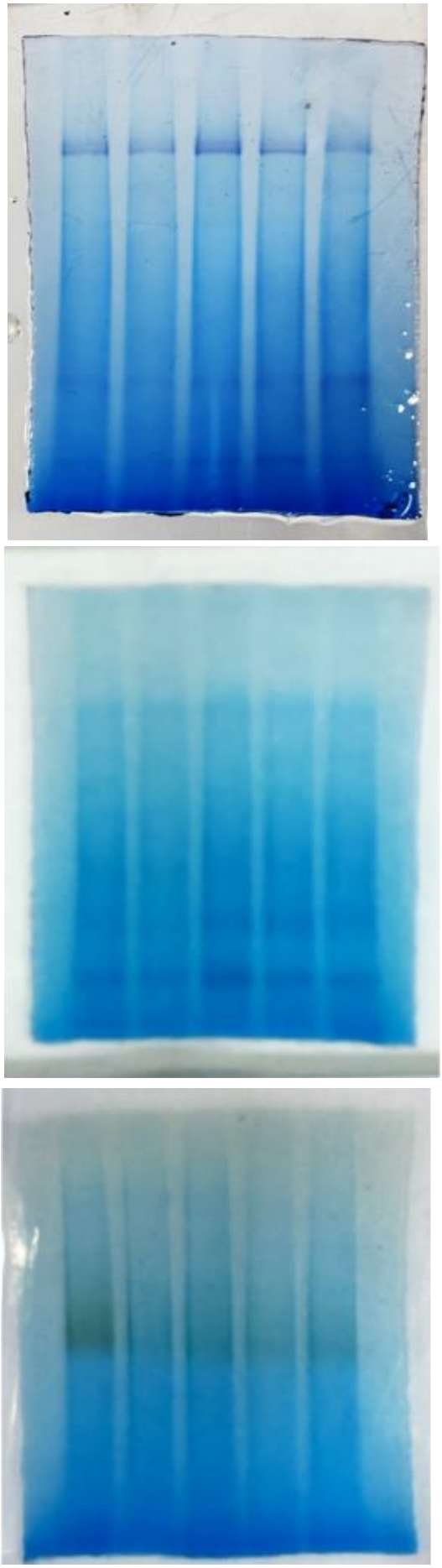

Uncropped images

Figure S8B

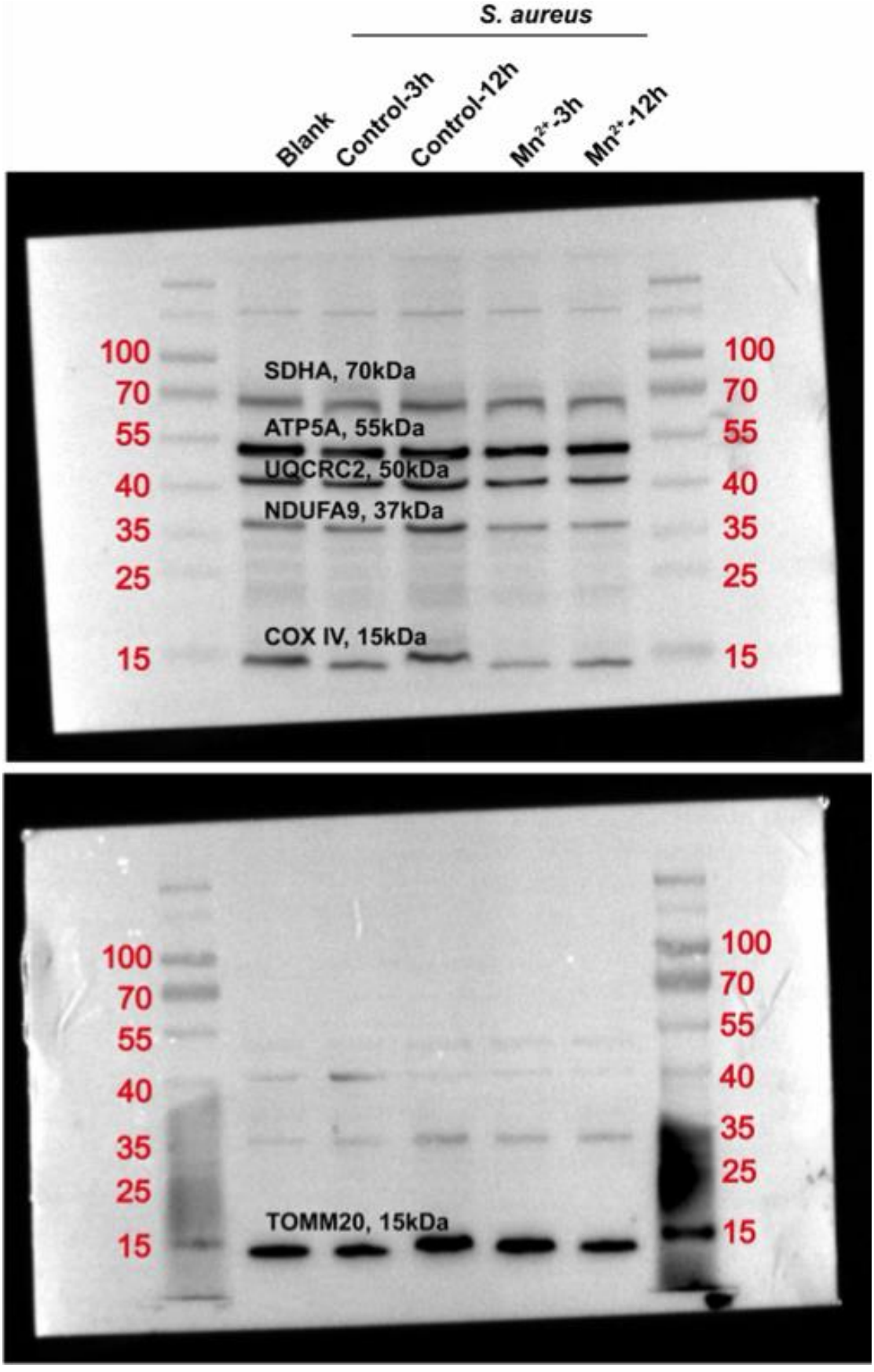

Uncropped images

Figure S9